

## A Study of the Star-forming Dwarf Galaxy NGC 855 with *Spitzer* \*

Sheng-Peng Li<sup>1</sup>, Qiu-Sheng Gu<sup>1</sup>, Ying-He Zhao<sup>1</sup>, Jia-Sheng Huang<sup>2</sup> and Xin-Lian Luo<sup>1</sup>

<sup>1</sup> Department of Astronomy, Nanjing University, Nanjing 210093; [sandaoren@163.com](mailto:sandaoren@163.com)

<sup>2</sup> Harvard-Smithsonian Center for Astrophysics, 60 Garden Street, Cambridge, MA 02138

Received 2007 March 21; accepted 2007 April 26

**Abstract** We present a study of the dwarf elliptical galaxy NGC 855 using the narrow-band  $H\alpha$  and *Spitzer* data. Both the  $H\alpha$  and *Spitzer* IRAC images confirm star-forming activity in the center of NGC 855. We obtained a star formation rate (SFR) of 0.022 and 0.025  $M_{\odot} \text{ yr}^{-1}$ , respectively, from the *Spitzer* IRAC 8.0  $\mu\text{m}$  and MIPS 24  $\mu\text{m}$  emission data. The HI observation suggests that the star-forming activity might be triggered by a minor merger. We also find that there is a distinct IR emission region in 5.8 and 8.0  $\mu\text{m}$  bands, located at about 10'' away from the nucleus of NGC 855. Given the strong 8.0  $\mu\text{m}$  but faint  $H\alpha$  emission, we expect that it is a heavily obscured star-forming region, which needs to be confirmed by further optical spectroscopic observations.

**Key words:** galaxies: elliptical — galaxies: individual: NGC 855

### 1 INTRODUCTION

Our understanding of early-type galaxies has dramatically improved during the last few decades. The standard scenario of the formation of elliptical galaxies was the monolithic collapse model, where elliptical galaxies formed the bulk of their stars in a single burst of star formation at high redshift, which evolved quietly and passively ever since, with very few new stars made in the past 1–2 Gyrs (Eggen, Lynden-Bell & Sandage 1962; Tinsley & Gunn 1976). On the other hand, the hierarchical, dissipative formation of elliptical galaxies suggested that massive galaxies form from the gradual merging of smaller galaxies, their present-day stellar mass was assembled at a recent epoch (e.g., White & Frenk 1991; Kauffmann, White & Guiderdoni 1993; Baugh, Cole & Frenk 1996). The numerical simulations have shown that major mergers of two disk galaxies or multiple successive minor mergers (with mass ratios larger than 3:1) can lead to the formation of “elliptical” remnants, which can be well fitted with the de Vaucouleurs’  $R^{1/4}$  law profile (Naab & Burkert 2003; Bournaud et al. 2006).

Different formation scenarios would predict different observed features for the elliptical galaxies, such as gaseous content, stellar population and surface brightness distribution, etc. In fact, there are several reports of the discovery of a large amount of cold gas/dust in elliptical galaxies: some ellipticals could have cold gas/dust as much as the spirals (Jura et al. 1987; Knapp et al. 1989; Caldwell 1984; Phillips et al. 1986; Lauer et al. 2005). Recently, Fukugita et al. (2004) and Zhao et al. (2006) reported their discoveries of active star-forming activities in the field elliptical galaxies in the Sloan Digital Sky Survey (SDSS), and that the percentage of such star-forming ellipticals amounts to about a few tenths. Fukugita et al. (2004) also suggested that these star-forming ellipticals could be the progenitors of E+A galaxies, interpreted as post-starburst galaxies that have terminated star-forming activity abruptly in the past 1–2 Gyr (Barger et al. 1996; Goto 2005).

NGC 855 is a fairly isolated elliptical galaxy (Lauberts 1982; de Vaucouleurs et al. 1991). Patchy dust structure was optically seen in the nuclear region (Ebner, Djorgovski & Davis 1988) as well

---

\* Supported by the National Natural Science Foundation of China.

as optical emission lines similar to Galactic HII regions (Maehara et al. 1987). Its redshift is 0.00198 (Simien & Prugniel 2000), which corresponds to a distance of 7.9 Mpc (for a Hubble constant of  $H_0 = 73 \text{ km s}^{-1} \text{ Mpc}^{-1}$ ,  $\Omega_M = 0.3$  and  $\Omega_\Lambda = 0.7$ ; 1 arcsec = 38 pc), the absolute blue magnitude ( $M_B$ ) is estimated to be  $-16.7 \text{ mag}$ . Thus, it should be classified as a star-forming dwarf elliptical galaxy. It was detected by IRAS at 12, 25, 60 and  $100 \mu\text{m}$  with flux densities of 0.077, 0.155, 1.145 and  $2.32 \text{ Jy}$ , respectively (IRAS Faint Source Catalogue, Moshir et al. 1990), therefore, the far-infrared luminosity from 40 to  $120 \mu\text{m}$ ,  $L_{\text{FIR}}$ , is about  $1.23 \times 10^8 L_\odot$ . Lees et al. (1991) derived the masses of atomic and molecular hydrogen gas in NGC 855 to be  $4.2 \times 10^7 M_\odot$  and  $(8.6 \pm 3.1) \times 10^5 M_\odot$ , respectively.

In this paper, we present the infrared data of NGC 855 from the *Spitzer Space Telescope* (Werner et al. 2004), where we discovered two distinct regions (separated by 10 arcsec) in the center of NGC 855. In order to study the physical nature of these two regions in detail, we also observed the narrow-band  $\text{H}\alpha$  image of NGC 855. We found that most of the  $\text{H}\alpha$  emission comes from the nuclear region, and that little  $\text{H}\alpha$  emission comes around the off-nuclear IR core. This paper is organized as follows: in Section 2 we present the *Spitzer* IRAC infrared images and narrow-band  $\text{H}\alpha$  images for NGC 855, and in Section 3 we derive the surface brightness and color distributions for the infrared images. Finally we discuss our results in Section 4 and draw conclusions in Section 5.

## 2 OBSERVATIONS AND DATA REDUCTION

A narrow-band  $\text{H}\alpha$  image of NGC 855 was obtained with the BAO Faint Object Spectrograph and Camera (BFOSC)<sup>1</sup>, attached to the 2.16 m telescope at the Xinglong Station of the National Astronomical Observatory, CAS. We used two narrow-band (on- and off- $\text{H}\alpha$  emission line) filters with band width of  $70 \text{ \AA}$  centered at  $6562 \text{ \AA}$  and  $6666 \text{ \AA}$ , respectively, during the observing run of Oct. 28–31, 2005. The exposure times for on- and off-band observations were the same, both were  $3 \times 3600 \text{ s}$ . Following Balogh & Morris (2000), we derived the narrow-band  $\text{H}\alpha$  image by removing the underlying continuum emission. All images were reduced using the standard IRAF<sup>2</sup> procedures.

NGC 855 is also one of 75 nearby galaxies observed by the *Spitzer* Legacy Program SINGS (Kennicutt et al. 2003). The IRAC images at 3.6, 4.5, 5.8 and  $8.0 \mu\text{m}$  for NGC 855 were downloaded from the Spitzer Science Center, which provides the Basic Calibrated Data (BCD) product with basic image processing, including dark subtraction, detector linearization corrections, flat-field corrections, and flux calibrations (see also the IRAC Data Handbook<sup>3</sup>). We further used the custom IDL software projecting the individual frame onto a uniform grid of 0.61 arcsec per pixel, conserving fluxes and rejecting outliers such as hot points of cosmic rays, and mosaicking as described by Huang et al. (2004). The flux calibration of IRAC extended sources, especially for elliptical galaxies, are presented by Jarrett<sup>4</sup>. Using the correction factors given by Jarrett, the resulting corrections, for the largest apertures, are about 0.08, 0.05, 0.20 and 0.26 mag, respectively for 3.6, 4.5, 5.8 and  $8.0 \mu\text{m}$  images. The final four IRAC bands have flux calibration accuracies of better than 10% (Fazio et al. 2004). Throughout this paper, all magnitudes are given in the AB system.

## 3 RESULTS

### 3.1 Central Star-forming Activity

Our narrow-band  $\text{H}\alpha$  image (Fig. 1d) indicates that the  $\text{H}\alpha$  emission comes mainly from the central region of NGC 855, which confirms the spectroscopic results by Maehara et al. (1987). Other lines of evidence for star-forming activity in the central nucleus of NGC 855 include the blue colors (Vila-Vilaró et al. 2003) and the weak extended non-thermal radio emission (Walsh et al. 1990). By using the empirical formulae provided by Kennicutt (1998), we can estimate the star formation rate (SFR) for NGC 855 from the  $\text{H}\alpha$ , infrared and radio data. The integral  $\text{H}\alpha$  emission line luminosity for the whole galaxy is  $L_{\text{H}\alpha} = 2.5 \times 10^{38} \text{ erg s}^{-1}$ , thus the corresponding  $\text{SFR}_{\text{H}\alpha}$  is equal to  $0.002 M_\odot \text{ yr}^{-1}$ . We can also use the far-infrared (FIR) luminosity derived from the IRAS 60 and  $100 \mu\text{m}$  fluxes,  $L_{\text{FIR}} = 1.23 \times 10^8 L_\odot$ , and the 1.4 GHz radio emission (Condon et al. 1998), both luminosities suggest that both  $\text{SFR}_{\text{FIR}}$  and  $\text{SFR}_{\text{Radio}}$  equal  $0.002 M_\odot \text{ yr}^{-1}$ .

<sup>1</sup> [http://www.xinglong-naoc.org/doc/BFOSManualv2\\_chinese.doc](http://www.xinglong-naoc.org/doc/BFOSManualv2_chinese.doc)

<sup>2</sup> IRAF is distributed by the National Optical Astronomy Observatories, which are operated by the Association of Universities for Research in Astronomy, Inc., under cooperative agreement with the National Science Foundation.

<sup>3</sup> <http://ssc.spitzer.caltech.edu/irac/dh/>

<sup>4</sup> <http://spider.ipac.caltech.edu/staff/jarrett/irac/calibration/index.html#res>

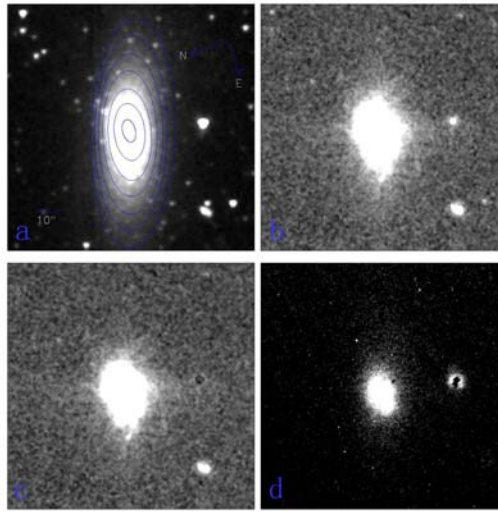


**Fig. 1** IRAC  $3.6\ \mu\text{m}$  (top left),  $8.0\ \mu\text{m}$  (top right), non-stellar  $8.0\ \mu\text{m}$  (bottom left) and  $\text{H}\alpha$  (bottom right) images of the dwarf elliptical galaxy NGC 855. The fitting elliptical isophotes are overlaid in the  $3.6\ \mu\text{m}$  image. The image sizes are  $\sim 2.2 \times 2.2$  arcmin.

The fact that the SFRs derived from  $\text{H}\alpha$ , FIR and radio emission are the same should be taken with great caution. The reasons are, (1) we did not perform the dust extinction correction for the integral  $\text{H}\alpha$  emission, as we did not have the  $\text{H}\beta$  information; (2) the NVSS 1.4 GHz radio emission is only from the central  $45''$  in NGC 855, thus both  $\text{H}\alpha$  and radio emission should underestimate the SFR in NGC 855.

In order to confirm such effects, we re-estimated the SFR from our IRAC  $8.0\ \mu\text{m}$  and MIPS  $24\ \mu\text{m}$  emission using the formulae given by Wu et al. (2006). Though the  $8.0\ \mu\text{m}$  band is dominated by the Polycyclic Aromatic Hydrocarbons (PAH) emission, there is still a non-negligible stellar contribution. Following Gu et al. (2007, in preparation) and Pahre et al. (2004), we made use of the IRAC  $3.6\ \mu\text{m}$  image to remove the stellar contribution in the  $8.0\ \mu\text{m}$  band. The non-stellar  $8.0\ \mu\text{m}$  image is shown in Figure 1c. From this image, we integrated and derived the  $8.0\ \mu\text{m}$  flux to be 47.65 mJy, the corresponding luminosity ( $\nu L_\nu(8\ \mu\text{m})$ ) is  $3.47 \times 10^7 L_\odot$ . Thus  $\text{SFR}_{8\ \mu\text{m}}$  is equal to  $0.022 M_\odot \text{yr}^{-1}$ . On the other hand, we can also estimate the SFR using the MIPS  $24\ \mu\text{m}$  emission, also provided by Wu et al. (2006). We integrated the MIPS  $24\ \mu\text{m}$  emission and derived the  $24\ \mu\text{m}$  flux of 67.5 mJy, giving  $\nu L_\nu(24\ \mu\text{m}) = 1.64 \times 10^7 L_\odot$ . We obtain that  $\text{SFR}_{24\ \mu\text{m}}$  is  $0.025 M_\odot \text{yr}^{-1}$ . The SFRs estimated from  $8.0\ \mu\text{m}$  and  $24\ \mu\text{m}$  emissions are consistent, both of which are one order of magnitude larger than those from the  $\text{H}\alpha$  and radio data, thus confirming that both  $\text{H}\alpha$  and radio data underestimated the SFR in NGC 855.

### 3.2 Infrared Radial Profiles

Following the methodology of Pahre (1999) and Pahre et al. (2004), we performed the task *ellipse* in IRAF to the  $3.6\ \mu\text{m}$  image, and derived all the elliptical isophotal information including the position of the center ( $x_0$  and  $y_0$ ), semi-major axis length, position angle and ellipticity, etc., that except for the center were then applied to the other three-band ( $4.5$ ,  $5.8$  and  $8.0\ \mu\text{m}$ ) images.

Figure 2 shows the radial surface brightness distribution for the *Spitzer* four-band ( $3.6$ ,  $4.5$ ,  $5.8$  and  $8.0\ \mu\text{m}$ ) images. We find that for the  $3.6$  and  $4.5\ \mu\text{m}$  images the surface brightness profiles can be well fitted by the de Vaucouleurs  $R^{1/4}$  profile. The minimum  $\chi^2$  of the fit by the de Vaucouleurs  $R^{1/4}$  law is typically 70% smaller than that by an exponential law. This result is consistent with Xilouris et al. (2004), where they found that for most elliptical galaxies of their sample, the  $4.5\ \mu\text{m}$  emission can be well described by a de Vaucouleurs profile. Though the  $5.8$  and  $8.0\ \mu\text{m}$  distributions in the inner  $20$  arcsec are significantly deviated from the  $R^{1/4}$  law, the surface brightness beyond  $20''$  can be well fitted with the de Vaucouleurs

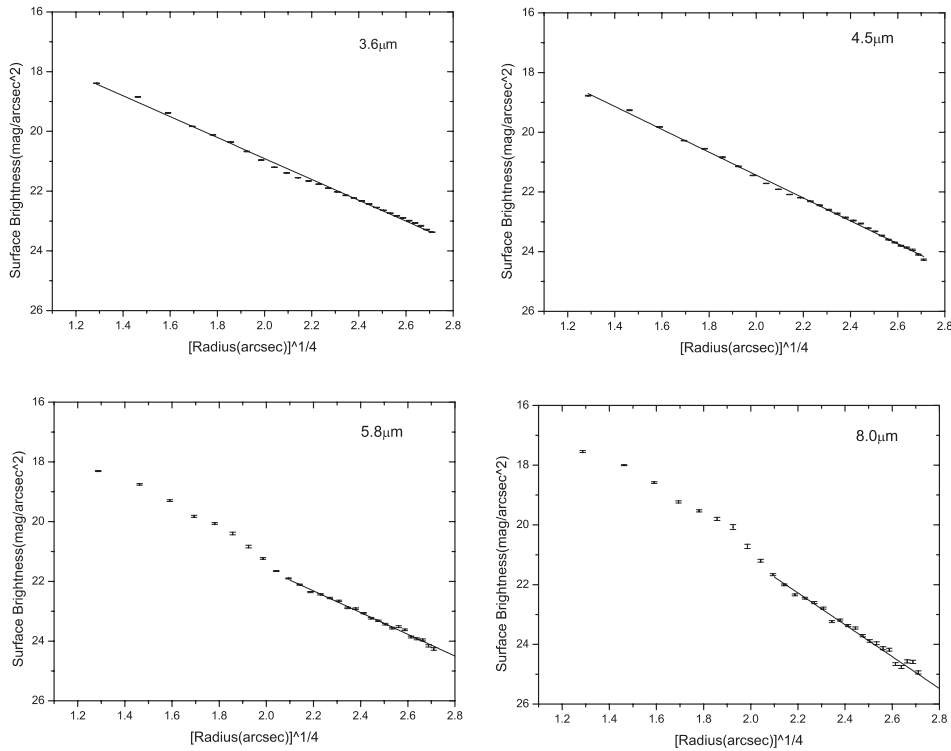


**Fig. 2** Surface brightness of NGC 855 as a function of radius for the IRAC 3.6, 4.5, 5.8 and 8.0  $\mu\text{m}$  images. The solid lines are the best fits with the  $R^{1/4}$  law. The error bar is shown for each measured point.

**Table 1** Results of fitting the surface brightness distribution with the de Vaucouleurs  $R^{1/4}$  law.

Band	$R_e$ arcsec	$\mu_e$ mag arcsec $^{-2}$	rms
3.6 $\mu\text{m}$	$32.13 \pm 1.40$	$22.23 \pm 0.09$	0.08
4.5 $\mu\text{m}$	$22.21 \pm 0.70$	$22.09 \pm 0.07$	0.07
5.8 $\mu\text{m}$	$27.60 \pm 2.41$	$22.65 \pm 0.20$	0.12
8.0 $\mu\text{m}$	$7.32 \pm 0.92$	$19.50 \pm 0.39$	0.19

law. The best fitting results by a de Vaucouleurs law are shown by the solid lines in Figure 2 and the fitting results are summarized in Table 1, including the effective radius ( $R_e$ ), the surface brightness ( $\mu_e$ ) of the isophote containing half the total light, and the rms values of the fitting.

As we know, the 3.6 and 4.5  $\mu\text{m}$  emissions trace the stellar mass distribution very well (Pahre et al. 2004), while the 5.8 and 8.0  $\mu\text{m}$  images contain rich information on the properties of the dust; the 8.0  $\mu\text{m}$  image in particular, with a passband centered at 7.9  $\mu\text{m}$ , includes some of the strongest emission features of PAHs (e.g. bands at 7.7 and 8.6  $\mu\text{m}$ ). Thus the deviations of the centers in the 5.8 and 8.0  $\mu\text{m}$  images confirm the current active star formation in the central region of NGC 855 as indicated in Section 3.1.

Following Pahre et al. (2004), we use the 3.6  $\mu\text{m}$  image to remove the stellar contribution in the other three IRAC images. In Figure 1, we show the IRAC 3.6, 8.0, non-stellar 8.0  $\mu\text{m}$  and the narrow-band H $\alpha$  images for NGC 855.

In Figure 3, the contour diagrams of the 3.6, 5.8, 8.0  $\mu\text{m}$  and narrow-band H $\alpha$  images are shown, respectively, in the upper left, upper right, lower left and lower right panels. It is interesting to note that 3.6  $\mu\text{m}$  and H $\alpha$  emissions come mainly from the nuclear region, and that while the 5.8 and 8.0  $\mu\text{m}$  emissions

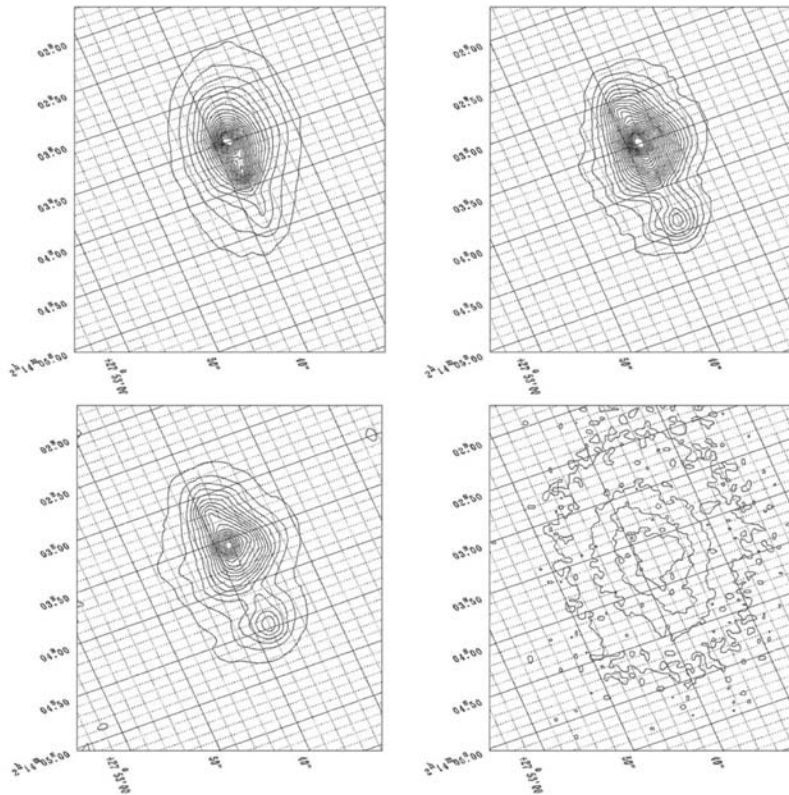


**Fig. 3** IRAC and  $H\alpha$  contour plots for NGC 855. The top panels show the  $3.6\ \mu\text{m}$  (left) and  $5.8\ \mu\text{m}$  (right) images, and the lower panels, the  $8.0\ \mu\text{m}$  (left) and  $H\alpha$  (right) images. Two distinct emission regions are unambiguously seen in the  $5.8\ \mu\text{m}$  (top right) and  $8.0\ \mu\text{m}$  (bottom left) images.

are also concentrated in the nuclear region, there is an additional and distinct emission region with little  $H\alpha$  emission, which is located at  $\sim 10''$  away from the nucleus. In Figure 4, we overlay the  $H\alpha$  emission contours on the  $8.0\ \mu\text{m}$  image.

#### 4 DISCUSSION AND CONCLUSIONS

We searched the NASA/IPAC Extragalactic Database (NED) in the field within  $30'$  of NGC 855 and did not detect any interacting companion. The isolated status of NGC 855 virtually excludes the possibility that the central star-forming activity is triggered by galaxy-galaxy interaction.

Walsh et al. (1990) observed the neutral hydrogen content in three elliptical galaxies (NGC 855, NGC 6958 and IC 1459) with strong far-infrared emission, and found that NGC 855 was the only one with detected HI 21 cm emission. The neutral gas in NGC 855 extended over 4 arcmin and was highly inclined to the optical major axis, with velocities indicative of a rotating gaseous disk, which might suggest that NGC 855 has experienced a recent minor merger.

By use of the Spitzer IRAC data, we find that the stellar profiles of  $3.6$  and  $4.5\ \mu\text{m}$  bands are well fitted by a  $R^{1/4}$  law, while deviations from the law exist in the central region in both  $5.8$  and  $8.0\ \mu\text{m}$  images. After removing the stellar emission, we find that there are two distinct emission regions (separated by  $\sim 10''$ ) in both  $5.8$  and  $8.0\ \mu\text{m}$  bands, but this is not seen in either the  $3.6\ \mu\text{m}$  or  $H\alpha$  images. Given the strong  $8.0\ \mu\text{m}$  and faint  $H\alpha$  emissions, we might expect that it is a heavily obscured star-forming region: optical spectroscopy should further constrain the underlying physical process.

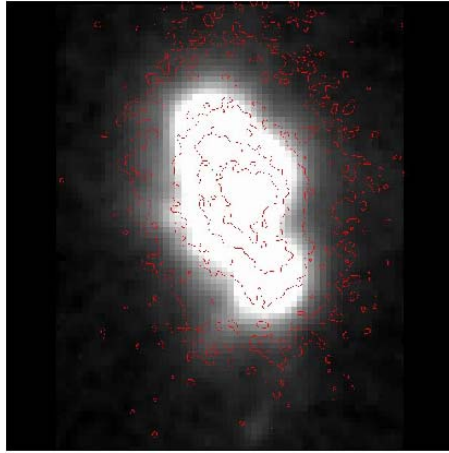


**Fig. 4** An  $H\alpha$  emission contour map is overlaid on the  $8.0\ \mu\text{m}$  emission image.

In this paper, we have presented the narrow-band  $H\alpha$  and Spitzer IRAC images of the dwarf elliptical galaxy NGC 855. Both the  $H\alpha$  image and the deviations of IRAC 5.8 and  $8.0\ \mu\text{m}$  distributions from the de Vaucouleurs profile confirm star-forming activity in the center of NGC 855. From the Spitzer IRAC  $8.0\ \mu\text{m}$  and MIPS  $24\ \mu\text{m}$  images, we derived the SFR in NGC 855 to be about  $0.02 M_{\odot} \text{yr}^{-1}$ . We also detected a distinct  $8.0\ \mu\text{m}$  emission region located at about  $10''$  away from the nucleus of NGC 855.

**Acknowledgements** We are very grateful to the anonymous referee for his/her thoughtful and instructive comments which significantly improved the content of the paper. This work is supported by the National Natural Science Foundation of China under Grants 10221001 and 10633040. QG would like to acknowledge the financial supports from the China Scholarship Council (CSC) and the Chinese Ministry of Education. We thank the Spitzer SINGS team for creation and distribution of the SINGS archive. This research has made use of the NASA/IPAC Extragalactic Database (NED) which is operated by the Jet Propulsion Laboratory, California Institute of Technology, under contract with the National Aeronautics and Space Administration.

## References

- Balogh M. L., Morris S. L., 2000, MNRAS, 308, 703  
 Barger A. J., Aragon-Salamanca A., Ellis R. S. et al., 1996, MNRAS, 279,  
 Baugh C. M., Cole S., Frenk C. S., 1996, MNRAS, 283, 1361  
 Bournaud F., Jog C. J., Combes F., 2005, A&A, 437, 69  
 Caldwell N., 1984, ApJ, 278, 96  
 Condon J. J., Cotton W. D., Greisen E. W. et al., 1998, AJ, 115, 1693  
 de Vaucouleurs G., de Vaucouleurs A., Corwin H. G. et al., 1991, Springer-Verlag: New York, Third Reference  
 Catalogue of Bright Galaxies (RC3)  
 Ebner K., Davis M., Djorgovski S., 1988, AJ, 95, 422  
 Eggen O. J., Lynden-Bell D., Sandage A. R., 1962, ApJ, 136, 748  
 Fazio G. G., 2004, ApJS, 154, 10  
 Fukugita M., Nakamura O., Turner E. L. et al., 2004, ApJ, 601L, 127  
 Goto T., 2005, MNRAS, 357, 937G  
 Huang J. S., Barmby P., Fazio G. G. et al., 2004, ApJS, 154, 44  
 Jura M., Kim D. W., Knapp G. R., Guhathakurta P., 1987, ApJ, 312, 11  
 Knapp G. R., Guhathakurta P., Kim D.-W., Jura M. A., 1989, ApJS, 70, 329  
 Kauffmann G., White S. D. M., Guiderdoni B., 1993, MNRAS, 264, 201  
 Kennicutt R. C. Jr., 1998, ARA&A, 36, 189

- Kennicutt R. C., Bendo G., Engelbracht C. et al., 2003, AAS, 203, 9010  
Lauberts A., 1982, fceu.book  
Lauer T. R., Faber S. M., Gebhardt K. et al., 2005, AJ, 129, 2138  
Lees J. F., Knapp G. R., Rupen M. P., Phillips T. G., 1991, ApJ, 379, 177  
Maehara H., Noguchi T., Takase B., 1986, AnTok, 21, 85, 550  
Moshir M., Kopan G., Conrow T. et al., 1990, BAAS, 22Q, 1325  
Naab T., Burkner A., 2003, ApJ, 597, 893  
Pahre M. A., 1999, ApJS, 124, 127  
Pahre M. A., Ashby M. L. N., Fazio G. G., Willner S. P., 2004, ApJS, 154, 235  
Phillips M. M., Jenkins C. R., Dopita M. A. et al., 1986, AJ, 92, 1062  
Simien F., Prugniel Ph., 2000, A&AS, 145, 263  
Tinsley B. M., Gunn J. E., 1976, ApJ, 203, 52  
visa-Vilaró B., Cepa J., Butner H. M., 2003, ApJ, 594, 232  
Walsh D. E. P., van Gorkom J. H., Bies W. E. et al., 1990, ApJ, 352, 532  
Werner M., Roellig T. L., Low F. J. et al., 2004, AAS, 204, 3301  
White S. D. M., Frenk C. S., 1991, ApJ, 379, 52  
Wu H. et al., 2005, ApJ, 632, L79  
Xilouris E. M., Georgakakis A. E., Misiriotis A., Charmandaris V., 2004, MNRAS, 355, 57X  
Zhao Y. H., Gu Q. S., Peng Z. X. et al., 2006, Chin. J. Astron. Astrophys. (ChJAA), 6, 15